# Ionization probability of sputtered atoms

N. D. Lang
*IBM Thomas J. Watson Research Center, Yorktown Heights, New York 10598*
(Received 21 September 1982)

The ionization probability of atoms sputtered from metal surfaces is discussed with the use of an approach of Blandin, Nourtier, and Hone. A general expression is obtained for this probability for the case in which the energy position of the sputtered-atom valence level has a linear dependence on distance and the atom velocity is constant. A limiting form of this expression was given by Brako and Newns; this limiting form is very useful in analyzing the higher-velocity part of the data obtained by Yu for $O^-$ sputtered from transition-metal surfaces. Analysis of the lower-velocity part of the data proceeds by the combination of the more general formulation of the theory with a very simple trajectory determined on the basis of a Morse-potential interaction between the sputtered adatom and the substrate atom which strikes it. A good account of Yu's experimental data is obtained with the use of parameter values determined solely from measurements and calculations of the ground-state properties of oxygen adsorbed on metal surfaces.

## I. INTRODUCTION AND GENERAL FORMULATION

We wish to consider in this paper the ionization probability of secondary atoms emitted from layers chemisorbed on a metal surface. We will use an approach discussed by Blandin, Nourtier, and Hone,[1] and later by Nørskov and Lundqvist[2] and Brako and Newns.[3] The metal is treated as a noninteracting Fermi gas of work function $\Phi$. We consider the interaction of the metal with a single atom, which is assumed to move along a classical trajectory $\vec{r}(t)$. The atom is taken to have a nondegenerate valence state $|a\rangle$ of energy $\epsilon_a$, lying in the metal conduction band. This level has a finite width because of its interaction with the states $|k\rangle$ of the metal, via matrix elements $V_{ak}=\langle a|V|k\rangle$, where $V$ is the perturbation due to the atom-metal interaction. Charge transfer between atom and metal is taken to involve the transfer of an electron between the broadened level $|a\rangle$ and metal states of the same energy. (We thus assume that Auger processes can be neglected relative to this resonant transfer process.[4])

Use of the trajectory approximation means that we can write $\epsilon_a$ and $V_{ak}$ in the electronic Hamiltonian as $\epsilon_a(\vec{r}(t))$ and $V_{ak}(\vec{r}(t))$, with $\vec{r}(t)$ the trajectory. Spin effects are neglected. The Hamiltonian is then written[5]

$$H(t)=\sum_k \epsilon_k n_k+\epsilon_a(\vec{r}(t))n_a + \sum_k [V_{ak}(\vec{r}(t))c_a^\dagger c_k+\text{H.c.}]\,, \tag{1}$$

where $c_a^\dagger$ and $c_k^\dagger$ are electron creation operators for $|a\rangle$ and $|k\rangle$, respectively, and $n=c^\dagger c$. Even though we will be interested in negative ions we do not take account of interactions of the form $Un_{a\uparrow}n_{a\downarrow}$ in $H$ (spin effects are omitted) because this would represent a major complication in the theory, and we wish instead to discuss the simplest possible model that gives a reasonable picture of the experimental data.

Following Ref. 1 the simplifying assumptions are made that the $k$ and $\vec{r}$ dependence of $V_{ak}(\vec{r}(t))$ are separable:

$$V_{ak}(\vec{r}(t))=V_k u(\vec{r}(t)) \tag{2}$$

and that the energy dependence of the level-width function

$$\Delta(\epsilon)=\pi\sum_k |V_{ak}|^2\delta(\epsilon-\epsilon_k) \tag{3}$$

can be neglected (this means in particular a constant substrate state density). The instantaneous resonance width is then given by

$$\Delta(\vec{r}(t))=\Delta_0|u(\vec{r}(t))|^2\,, \tag{4}$$

where we take $|u|^2=1$ for $t=0$. Note that $\Delta$ is the halfwidth at half maximum of the adsorbate resonance. With these assumptions, the occupation probability $\langle n_a(t)\rangle$ has been obtained by Blandin, Nourtier and Hone,[1] and subsequently by Brako and Newns.[3] In particular, for $t\to\infty$ (setting $\hbar=1$),

 

$$P\equiv\langle n_a(\infty)\rangle=\langle n_a(0)\rangle\exp\left[-2\int_0^\infty\Delta(\vec{r}(t))dt\right]$$
$$+\frac{1}{\pi}\int_{-\infty}^{\epsilon_F}d\epsilon\left|\int_0^\infty dt[\Delta(\vec{r}(t))]^{1/2}\exp\left[i\epsilon t+\int_t^\infty[i\epsilon_a(\vec{r}(t'))-\Delta(\vec{r}(t'))]dt'\right]\right|^2. \quad (5)$$

[We omit from Eq. (5) a "cross" term[6] that is negligible in all cases of interest here.] Since[7]

$$\int_{-\infty}^{\epsilon_F}e^{ix\epsilon}d\epsilon=\pi\delta(x)+\frac{e^{ix\epsilon_F}}{ix}, \quad (6)$$

if we write

$$f(t)\equiv\left[\frac{\Delta(\vec{r}(t))}{\Delta_0}\right]^{1/2}\exp\left[-\int_t^\infty\Delta(\vec{r}(t'))dt'\right], \quad (7)$$

then

$$P=\langle n_a(0)\rangle f^2(0)+\Delta_0\int_0^\infty f^2(t)dt+\frac{\Delta_0}{\pi}\int_0^\infty dt\int_0^\infty dt'f(t)f(t')\frac{\sin\int_t^{t'}[\epsilon_F-\epsilon_a(\vec{r}(t''))]dt''}{t'-t}. \quad (8)$$

This form is used for the numerical calculations that we do later. The first term here is often negligible in the experimental parameter range.

We will neglect any dependence parallel to the surface, and take $\Delta$ and $\epsilon_a$ to depend only on $z$, the coordinate along the surface normal. We also use a simple exponential form for $\Delta$:

$$\Delta(z)=\Delta_0e^{-\gamma z} \quad (9)$$

(we take the atom position at $t=0$ to be $z=0$).

## II. RESULT FOR THE CASE OF CONSTANT VELOCITY AND LINEAR $\epsilon_a(z)$

Blandin, Nourtier, and Hone[1] have given an analytic evaluation of $P$ using the above assumptions, and further assuming that $z=v_\perp t$ and that $\epsilon_a$ is a constant distance from the Fermi level. They neglect terms of $O(e^{-\Delta_0/\gamma v_\perp})$, which is in most instances a good approximation. We give here the solution for the case in which $\epsilon_a$ crosses the Fermi level, which is generally the case of greater interest. In particular, we take

$$\epsilon_a(z)=\epsilon_F+b(z-z_c) \quad (10)$$

with $z_c$ the distance at which the level crosses $\epsilon_F$. Again with $z=v_\perp t$ and neglecting terms of $O(e^{-\Delta_0/\gamma v_\perp})$ (see Appendix A for details, where the result that includes these neglected terms is given),[8]

$$P=\tfrac{1}{2}+\frac{\zeta}{\pi}\,\mathrm{Re}\int_0^\infty\frac{dx}{\cosh x}\left[\frac{2\Delta_0}{\gamma v_\perp}\cosh x\right]^{i\zeta x}$$
$$\times e^{-i\zeta\gamma z_c x}\Gamma(-i\zeta x), \quad (11)$$

where

$$\zeta=\frac{2b}{\gamma^2v_\perp}. \quad (12)$$

In the limit in which $\zeta\to\infty$ (see Appendix A),

$$P\to e^{-2\Delta(z_c)/\gamma v_\perp}. \quad (13)$$

This limit has been obtained by Brako and Newns.[3] Comparison with the result in Eq. (11) shows this limiting form to be quite accurate for many cases of interest. For example, for a set of parameters appropriate to the case of $O^-$ sputtered from vanadium described below, over the velocity range in the experiment [$(0.5-3)\times10^6$ cm/sec], Eq. (13) is accurate to better than 1% [the parameter $\zeta$ is $O(10^2)$]. We will find this form very useful for our qualitative discussion.

## III. EXPERIMENTAL DATA ON $O^-$; MORE REALISTIC FORM FOR $\epsilon_a(z)$

We wish now to discuss the experimental data of Yu[9] for $O^-$ sputtered from a vanadium substrate. These experiments measure changes in $\ln Y^-$ ($Y^-$ is the negative ion yield) that occur as the substrate work function is changed by depositing an alkali layer. A curve of $\log_{10}Y^-$ versus change in $\Phi$ is shown in Fig. 1; it is seen to be linear over a considerable range. An energy parameter $\epsilon_0$ is then defined from the slope of such a curve (in the linear region),

$$\epsilon_0=-\left[\frac{d\ln Y^-}{d\Phi}\right]^{-1}, \quad (14)$$

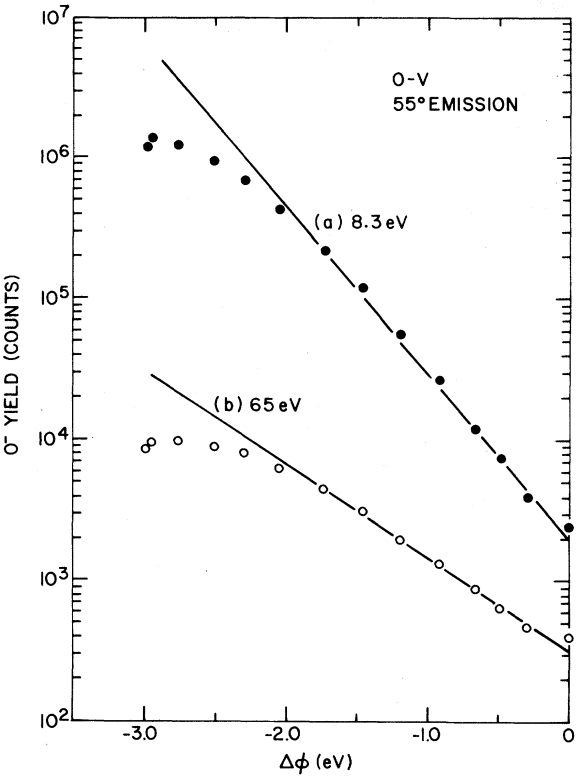


FIG. 1. Work-function dependence of yield of $O^-$ ions sputtered from a vanadium surface at two different emission energies, (a) 8.3 and (b) 65 eV, but for the same angle of emission, as measured by Yu (from Ref. 9). The surface was exposed to 1 L of oxygen. Changes in work function $\Delta\Phi$ are brought about by deposition of submonolayers of Li on the surface.

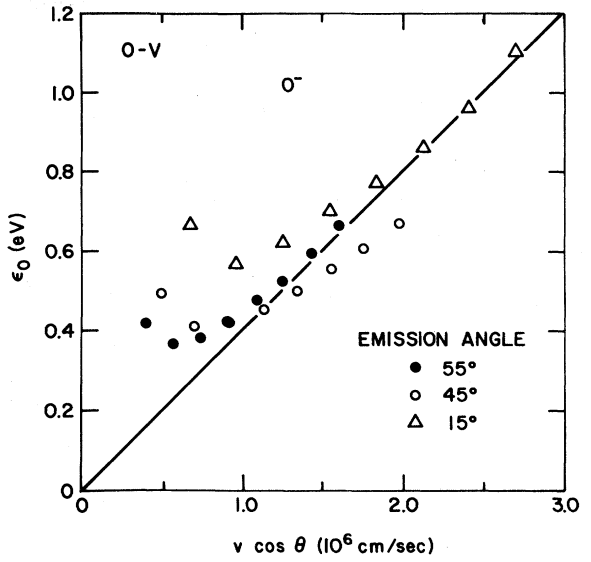


FIG. 2. Dependence of $\epsilon_0$ for $O^-$ sputtered from oxygenated (1 L) vanadium surfaces on the normal component $v_\perp$ of the emission velocity, as measured by Yu (Ref. 9). Straight line was drawn to show proportionality of $\epsilon_0$ to $v_\perp$ at large $v_\perp$. The position of the uppermost triangle data point was incorrectly plotted in Ref. 9; the error is corrected in the figure given here (Ref. 14).

and is plotted as a function of measured velocity perpendicular to the surface for several emission angles as shown in Fig. 2. This procedure is viewed in Ref. 9 as assuming that

$$Y^- \propto e^{-(\Phi - A)/\epsilon_0} \tag{15}$$

($A$ is the affinity energy of the sputtered atom). The proportionality constant here involves mechanical factors relating to, e.g., the sputtering coefficient (number of sputtered atoms per incident ion). Extraction of $\epsilon_0$ eliminates this complicated proportionality factor. We can thus obtain values for $\epsilon_0$ directly from the calculated probabilities $P$:

$$\epsilon_0 = -\left[\frac{d \ln P}{d\Phi}\right]^{-1} . \tag{16}$$

Now we note several features of the experimental data given in Figs. 1 and 2.

(1) The curve of $\ln Y^-$ vs $\Phi$ is linear over a large range.

(2) The curve of $\epsilon_0$ vs $v_\perp$ is linear for large $v_\perp$.

(3) $\epsilon_0$ vs $v_\perp$ shows a minimum at small $v_\perp$.

(4) The smaller the emission angle, the larger the $\epsilon_0$ and $v_\perp$ at which the minimum occurs.

(5) For the near-normal incidence curve, the minimum occurs for an emitted ion kinetic energy approximately equal to the heat of ionic desorption of $O^-$ from an oxygen-covered vanadium surface.

We will try to understand the origin of these features and will attempt to give a quantitative account of the data using only parameters that describe the ground state of the oxygen-vanadium adsorption system, obtained from both measurements and calculations.

To proceed with our discussion, we must choose a form for $\epsilon_a(z)$ that describes its basic behavior somewhat more accurately than the simple linear form of Eq. (10). Reference 10 argues that the energy position of the valence-state resonances of chemisorbed atoms follows the total surface barrier potential, as a function of distance. In the immediate surface region, this potential has an exponential behavior, and so we take this to be the form of $\epsilon_a(z)$. Figure 3 illustrates this approximate behavior over a short range in the surface region (the arrows in the figure give the value of the surface potential). For the negative ions we discuss here, $\epsilon_a(z)$ must tend to

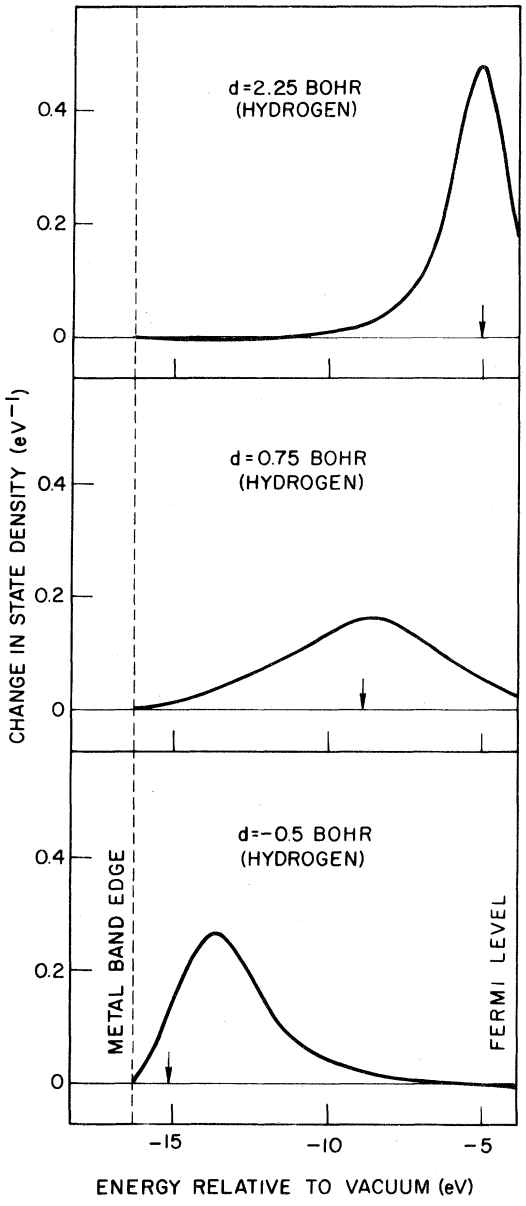


FIG. 3. Self-consistently calculated state-density change due to chemisorption of a hydrogen atom on a high-density metallic substrate (jellium model). Curves are shown for three different metal-adatom distances $d$ (measured from the positive background edge of the model substrate). Arrow gives value of total surface potential at adatom nucleus; zero is set so that arrow falls under peak of resonance for largest distance. This shows the way in which the resonance position roughly follows the surface potential. Note the nonmonotonic behavior of the resonance width with distance. Curves are from Ref. 10.

$-A$ for $z\to\infty$, with $A$ the affinity energy of the free atom. We therefore write, approximately,

$$\epsilon_a(z)=Ce^{-\alpha z}-A \tag{17}$$

(with the vacuum taken as the zero of energy).

In fact, we expect that $\epsilon_a(z)$ will have an image-like dependence on distance far from the metal, but for electronegative atoms such as oxygen, whose resonances are generally well below the Fermi level in equilibrium, the bulk of the variation occurs closer to the surface, where the behavior is exponential. For such atoms, therefore, in the interest of simplicity, we neglect this imagelike behavior. We note also that far from the surface, the behavior is exponential with $\alpha\propto\sqrt{\Phi}$ in, e.g., a local-density calculation (which by its nature does not include image effects), but that would be far enough out that the true behavior would be imagelike and not exponential in any case. We therefore neglect any work-function dependence of $\alpha$. We will further assume that the distance below the Fermi level of $\epsilon_a(z)$ for the atom at equilibrium (defined to correspond to $z=0$), i.e.,

$$E_0=\epsilon_F-\epsilon_a(0)\ , \tag{18}$$

is also independent of $\Phi$.[11]

The quantity that enters Eq. (8) for $P$ is

$$\epsilon_F-\epsilon_a(z)=(\Phi-A+E_0)e^{-\alpha z}-(\Phi-A) \tag{19}$$

(note that $\epsilon_F=-\Phi$). The distance $z_c$ at which $\epsilon_a(z)$ crosses the Fermi level [i.e., $\epsilon_a(z_c)=\epsilon_F$] is given by

$$z_c=\frac{1}{\alpha}\ln\frac{\Phi-A+E_0}{\Phi-A}\ . \tag{20}$$

## IV. SIMPLIFIED ANALYSIS OF EXPERIMENTAL DATA

Now, solely for purposes of discussion, we will use the above expression for $z_c$ in conjunction with the limiting form for $P$ given in Eq. (13), which was derived for a linear potential. We do this because we expect that it is only the region near the crossing point which is important in obtaining Eq. (13), over which our form (19) is locally linear. In this case, continuing to take $z=v_\perp t$, we have

$$P=\exp\left[-\frac{2\Delta_0}{\gamma v_\perp}\left[\frac{\Phi-A}{\Phi-A+E_0}\right]^{\gamma/\alpha}\right]\ . \tag{21}$$

If we crudely take $\gamma\sim\alpha$, then we can write this as

$$P\approx e^{-(\Phi-A)/\epsilon_0} \tag{22}$$

with

$$\epsilon_0=\frac{\alpha}{2\Delta_0}(\Phi-A+E_0)v_\perp \tag{23}$$

[we take Eq. (15) rather than (16) to define $\epsilon_0$ for the moment]. Since for a negative ion such as oxygen, $E_0$ is relatively large [$\sim$6 eV (Ref. 12)] and since $\Phi\sim 5$ eV, we can neglect variations in $\epsilon_0$ due to changes in $\Phi$ of $\sim$1–2 eV. We understand in this manner the way in which Eq. (22) implies the approximate linearity of the curve of $\log_{10}Y^-$ vs $\Phi$ over a range of $\sim$2 eV seen in Fig. 1.

We now return to the somewhat more accurate form Eq. (21), which implies [from Eq. (16)]

$$\epsilon_0=\frac{\alpha}{2\Delta_0}\frac{(\Phi-A+E_0)^{\gamma/\alpha+1}}{E_0(\Phi-A)^{\gamma/\alpha-1}}v_\perp\,, \tag{24}$$

and discuss the actual values of the parameters. Note that Eq. (24) [and (23) as well] reflects the linearity of the curve of $\epsilon_0$ vs $v_\perp$ seen in Fig. 2 for high velocities.

We consider the system of $\sim$1 L (langmuir) oxygen adsorbed on polycrystalline vanadium analyzed by Yu,[9] the results for which are given in Figs. 1 and 2. First we discuss the parameters that are the most straightforward to determine. The work function of polycrystalline vanadium is 4.3 eV (Ref. 13); the work-function change induced by 1 L of oxygen is 0.9 eV as measured by Yu.[14] We thus take $\Phi=5.2$ eV. The affinity energy for oxygen is 1.5 eV (Ref. 15) (to the accuracy of interest here). The value of $E_0$ is found in photoemission experiments to be $\sim$6 eV.[12] The inverse decay length $\alpha$ for the surface barrier potential on a high-density metal substrate is calculated[16] to be $\sim$0.4 bohr$^{-1}$; as argued above this should be the characteristic inverse decay length for the resonance position $\epsilon_a(z)$ also.

The parameters that are more difficult to determine are $\Delta_0$ and $\gamma$. Note in Fig. 3 that the resonance width is not a monotonic function of the distance of the atom from the surface. This is due to the fact that as the atom is moved toward the metal, the atom-metal overlap increases, causing the resonance to widen, but at the same time the resonance position moves down in energy causing the density of metal states with which the atomic resonance is degenerate to decrease (it of course becomes zero at the bottom of the metal band), leading to a decrease in the resonance width. The nonmonotonic behavior results from a competition between these two effects [cf. Eq. (3)]. In many cases, it is thus not appropriate to use the measured $\Delta_0$ (the halfwidth at the atom equilibrium position) because the resonance will often widen somewhat when the atom is moved outward from equilibrium. Instead, we will use the maximum value of $\Delta(z)$ as calculated by Lang and Williams[10,17] using the atom-jellium model. For oxygen on a high-density metal, this is $\sim\frac{3}{2}$ eV [the value that is measured for oxygen adsorbed on a transition metal surface at its equilibrium distance is $\sim$1 eV (Ref. 12)]. We should of course note that the derivation of Eq. (5) assumed the substrate density of states to be constant in energy, i.e., took $\Delta$ to be energy independent, so treating the actual problem in the way just described represents an approximation for this reason as well. Because of the complex behavior of the resonance width, there is some uncertainty as to the proper way to extract a value of $\gamma$, whose definition is based on assuming the simple monotonic behavior of Eq. (9). If we fit the behavior of the oxygen resonance width as a function of position (as calculated in the atom-jellium model) to an exponential over the range from $\sim\frac{1}{2}$ bohr outside the position of maximum width to $\sim\frac{5}{2}$ bohr outside (the largest distance for which calculations were performed), then a value $\gamma\sim 0.5$ bohr$^{-1}$ is obtained. If we fit only the behavior near the outermost calculated distances, we obtain $\gamma\sim 0.7$ bohr$^{-1}$.

Evaluating Eq. (24) using the parameter values given above yields (oxygen on vanadium)

$$\epsilon_0=0.1(11^\gamma)v_\perp\quad(\gamma\sim 0.5\text{–}0.7)\,. \tag{25}$$

($\epsilon_0$ is in units of eV, and $v_\perp$ is in units of $10^6$ cm/sec.) This result is graphed for two values of $\gamma$ together with Yu's data in Fig. 4. We see from this that a completely *a priori* determination of the parameters gives a reasonable account of the high-velocity behavior.

Yu[9] has also measured $\epsilon_0$ for oxygen adsorbed on Nb, and has found the slope of the $\epsilon_0$ vs $v_\perp$ curve at large $v_\perp$ to be about $\frac{3}{4}$ that of the O-V case. Within the picture described above, and to the accuracy with which we have determined the parameters for oxygen adsorbed on vanadium, the two cases should differ only in the value of $\Phi$ employed. Now the work function of polycrystalline Nb is the same as that of V (4.3 eV),[13] but the work-function increase induced by 1 L of oxygen on Nb is $\lesssim$0.1 eV in Yu's experiment,[14] in contrast to the much larger change observed for adsorption on *V*. We thus use a value $\Phi=4.4$ eV. The numerical expression for $\epsilon_0$ in this case is then (oxygen on niobium)

$$\epsilon_0=0.07(16.5^\gamma)v_\perp\quad(\gamma\sim 0.5\text{–}0.7)\,. \tag{26}$$

($\epsilon_0$ is in units of eV and $v_\perp$ is in units of $10^6$ cm/sec.) This result is graphed in Fig. 5 for the same two values of $\gamma$ shown in Fig. 4, together with Yu's data. The agreement at higher velocities is again adequate.

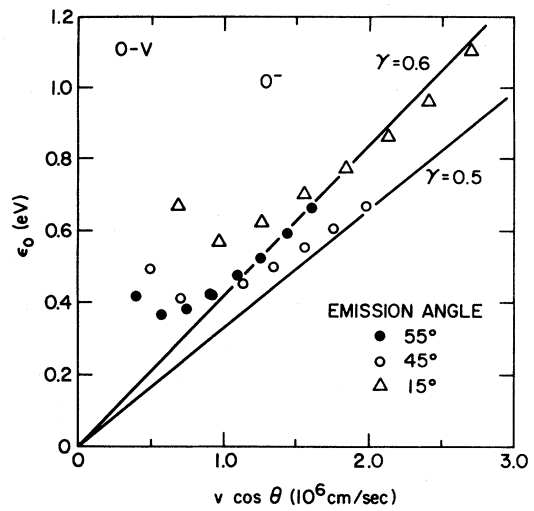


FIG. 4. Experimental data of Yu (Ref. 9) for $O^-$ sputtered from oxygenated (1 L) vanadium surfaces shown in Fig. 2, compared with the simple approximation given by Eq. (25).

## V. ANALYSIS OF EXPERIMENTAL DATA USING MORE REALISTIC TRAJECTORY

In order now to discuss the low-velocity behavior of $\epsilon_0$ in Fig. 2, i.e., the region where the behavior deviates from linearity, we must consider somewhat more carefully the classical trajectory $\vec{r}(t)$ of the emitted ion. Since the atom is in a potential well near the surface, its velocity in this region must be larger than the measured velocity $v$ far from the surface. Since the average velocity over the trajectory will thus be larger than $v$, and since $\epsilon_0$ increases (linearly) with $v$ in our simple model, we expect for $v$ small enough that the velocity increase in the well region is comparable to $v$ itself that $\epsilon_0$ will be increased, relative to the value obtained from our simple model (which omitted the well). This is of course what is seen in Fig. 2.

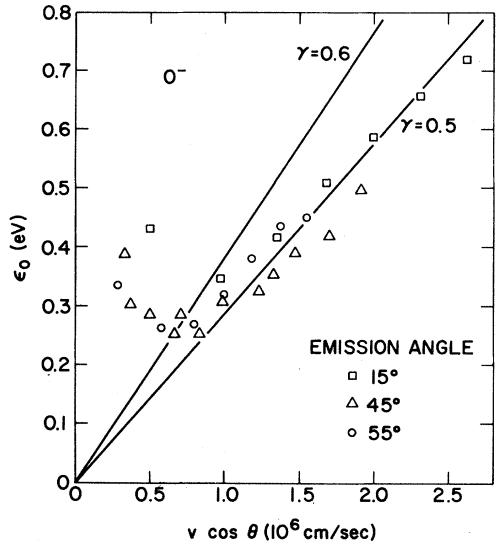


FIG. 5. Experimental data of Yu for $O^-$ sputtered from oxygenated (1 L) Nb surfaces from Ref. 9, compared with the simple approximation given by Eq. (26).

To discuss this in a somewhat more quantitative way, we will evaluate $P$ (and hence $\epsilon_0$) numerically, evaluating Eq. (8) for an appropriate trajectory. We continue to take $\epsilon_0$ and $\Delta$ to depend only on the perpendicular distance of the particle from the surface, i.e., on the component $z(t)$ of the trajectory $\vec{r}(t)$.[18] We retain the simple exponential forms for $\Delta(z)$ [Eq. (9)] and $\epsilon_a(z)$ [Eq. (19)].

We will use a highly simplified picture to obtain a trajectory, in order to explore some of the general aspects of the experimental data, without pretending to a comprehensive treatment of the problem. We consider the adsorbed atom that is leaving the surface to have been struck by a single substrate atom. We take the interaction potential between the two to have a Morse form

$$U(s)=\mathscr{E}(1-e^{-\beta(s-s_0)})^2-\mathscr{E} \tag{27}$$

with $s$ the bond length ($s_0$ at equilibrium). We imagine that at time $t=0$ the substrate atom receives a sudden impulse and that it then, with no further interactions with other substrate atoms, collides head-on with the adsorbed atom (i.e., zero impact parameter). The adatom then moves out along the line of collision, which is at an angle $\theta$ with respect to the surface normal. All interactions with atoms other than the one that struck it, including the effects of, e.g., image attraction on the trajectory, are neglected. This is clearly a highly simplified picture, but we find that it elucidates a sufficient part of the experimental data to make it worth discussing.

Let us denote the mass of the adsorbed atom by $m$, and that of the substrate atom by $M$. For the cases of interest here, $M$ is several times as large as $m$. Since the data discussed here are for sputtered adatoms with energies in the range 5–200 eV, we expect that in most cases the substrate atom will have had enough energy to leave the surface also.

Let us denote by $v_M$ the velocity of the substrate atom at $t=0+$, i.e., just after it has received a sudden impulse from the remainder of the substrate. We write also

$$v_{\mathscr{E}} \equiv \left[\frac{2\mathscr{E}}{m(1+\delta)}\right]^{1/2}, \tag{28}$$

with mass ratio

$$\delta \equiv \frac{m}{M} . \tag{29}$$

Now for $v_M > v_{\mathscr{E}}(1+\delta)$, the distance between the substrate atom and the sputtered adatom increases monotonically with time; and the adatom arrives by itself at the detector as $t \to \infty$ (Appendix B). We denote by $v$ its velocity at the detector. We can for this case write the condition on the substrate-atom velocity, $v_M > v_{\mathscr{E}}(1+\delta)$, as a condition on the velocity of the sputtered atom at the detector: $v > v_{\mathscr{E}}$. (See Appendix B for details.)

For $v_M < v_{\mathscr{E}}(1+\delta)$, the solution changes character, with $s$ a periodic function of time. Thus the sputtered adatom and the moving substrate atom remain bound to each other. Since the experiment of Yu which we wish to consider mass filters the secondary ions with a quadrupole mass spectrometer, we will assume that such dimers have been eliminated, and will therefore not consider such trajectory solutions.

We now evaluate Eq. (8) numerically using the trajectory given in Eq. (B12), for the sputtering of oxygen from vanadium. We use the same set of parameters employed in our prior discussion of this case, taking $\gamma = 0.6$ bohr$^{-1}$ (see Fig. 4). The value of $m$ for this case is 16 atomic mass units, and the mass ratio $\delta$ is 0.31.

The additional parameters that must be discussed are those of the Morse potential, $\mathscr{E}$ and $\beta$. A value for $\beta$ can be obtained from vibrational properties of diatomic molecules[19]; the data for VO give $\beta \sim 1$ bohr$^{-1}$. We take $\mathscr{E}$ to be the heat of ionic desorption of, in the present case, an $O^-$ ion on a vanadium surface with 1 L of oxygen. Doing this goes outside of our procedure of considering only an adatom-substrate atom pair and not considering the remainder of the substrate. The energy to dissociate a VO diatomic into $V^+$ and $O^-$, however, seems inappropriate to consider in the present problem, particularly the part of the energy that can be ascribed to a transfer of an electron from a single V atom (as contrasted with the entire substrate) to the O atom.

The heat of adsorption of an O on a transition-metal surface with monolayer oxygen coverage is in the range 4–6 eV.[20] To obtain the heat of ionic adsorption, we must add to this $\Phi - A = 3.7$ eV for our case. We thus take $\mathscr{E} \sim 9$ eV. We note that the results are not extremely sensitive to the exact value of $\mathscr{E}$, and would not be radically different even if we had in fact used for $\mathscr{E}$ the energy to dissociate a VO diatomic into $V^+$ and $O^-$ [11.7 eV (Ref. 19)].[21]

Values for $P$ were obtained for the work function $\Phi$ (whose value was given earlier as 5.2 eV) and for $\Phi - 1$ eV, and a value for $\epsilon_0$ was obtained from Eq. (16). The use of a 1-eV difference as an approximation to the derivative corresponds most closely to the experimental procedure of drawing curves like those of Fig. 1 and taking the slope of the initial 1–2 eV section to extract $\epsilon_0$. (A plot of the calculated $P$ vs $\Phi$ does in fact show it to be quite linear over such a range.) We note that the contribution of the first term in Eq. (8) to $P$ is negligible over the velocity range considered in the experiments.

Results are shown in Fig. 6 for two of the emission angles measured by Yu[9] [the angle enters via Eq. (B12)]. The calculated curves are seen to reproduce the general behavior of the experimental data for velocities $v_\perp$ greater than that at which the minimum occurs in the measured value of $\epsilon_0$. Note that the calculated curves are begun at a perpendicular velocity $v_\perp = v_{\mathscr{E}} \cos\theta$, below which (as noted earlier) the sputtered atom and the adsorbate atom (which we presume has left the surface) remain bound to each other. Figure 6 strongly suggests that this point should be identified with the minimum in the experimental curves. The present simple model does not seem adequate to explain the observed rise in $\epsilon_0$ as $v_\perp$ drops below this point; a more sophisticated treatment of the mechanics (e.g., considering collisions with a statistical distribution of impact parameters) is presumably required.

Figure 6 compares theory and experiment for the $\theta = 15°$ and $\theta = 55°$ data from Fig. 2. The fact that the experimental curve in Fig. 2 for $\theta = 45°$ appears

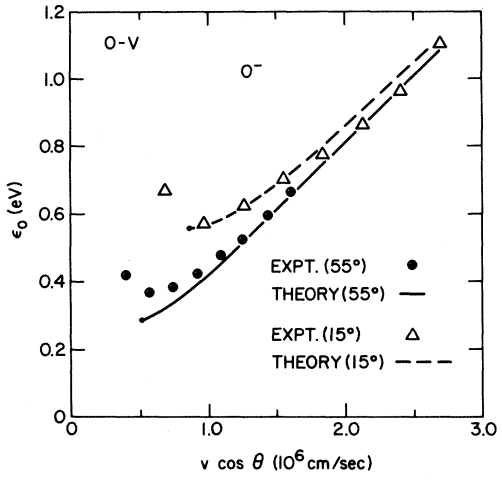


FIG. 6. Experimental data of Yu (Ref. 9) for $O^-$ sputtered from oxygenated (1 L) vanadium surfaces, for emission angles of 15° and 55°, shown in Fig. 2, compared with results obtained from a numerical evaluation of Eq. (8) for the trajectory of Eq. (B12). The value 0.6 bohr$^{-1}$ is used for the resonance-width inverse decay length $\gamma$ (cf. Fig. 4). Calculated curves terminate at the low-velocity end in a dot that marks the positions $v = v_{\mathscr{E}}$ discussed in the text.

to have a different slope at large velocities from the other two curves seems hard to understand on general grounds and the theoretical curve for 45° does not, of course, reproduce this behavior. (It is simply an interpolation between the two curves already given in Fig. 6.)

Figure 7 shows the calculated $P$ values directly, versus $1/v_\perp$. Such plots emphasize the deviation at low velocities from the simple linear behavior found at higher velocities. In the limit $1/v_\perp \to 0$ (the sudden limit), $\ln P \to \ln\langle n_a(0)\rangle$, with $\langle n_a(0)\rangle = 0.92$ for our case.[22] (Recall that we consider here only a single adatom orbital with no spin degeneracy, and thus $0 \le \langle n_a \rangle \le 1$.)

We should conclude by noting that the theory presented here is directly applicable to the sputtering of position ions, both from adsorbate layers[23] and of course from clean metals as well. For the case of sputtered adsorbed alkalis, e.g., one important difference is just that $E_0$ is negative and the affinity energy $A$ is replaced by $I$, the ionization potential. The other important difference arises from the fact that the equilibrium position of an alkali is much further out than that of a small electronegative atom like oxygen, which leads to a situation in which the imagelike behavior of $\epsilon_a(z)$ is much more important than its exponential component.

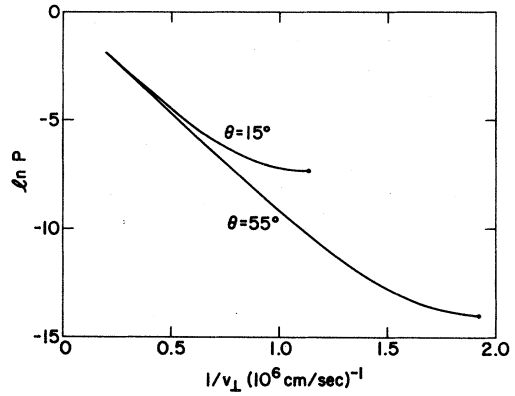


FIG. 7. Calculated curves of $\ln P$ vs $1/v_\perp$ for $O^-$ sputtered from a surface with $\Phi = 5.2$ eV [corresponding to an oxygenated (1 L) vanadium surface before an alkali submonolayer is deposited]. The same calculational procedure and parameters are used here as were employed to obtain Fig. 6.

## ACKNOWLEDGMENTS

I am delighted to acknowledge useful discussions with M. L. Yu, D. W. Jepsen, C. H. Bennett, and J. K. Nørskov.

## APPENDIX A: RESULTS FOR THE CASE OF LINEAR $\epsilon_a(z)$

We consider in this appendix the evaluation of Eq. (8) for $P$ for the simple case in which $z = v_\perp t$, $\Delta(z)$ has the exponential decay given in Eq. (9), and $\epsilon_a(z)$ has the linear behavior given in Eq. (10).

In this instance, the function $f(t)$ defined in Eq. (7) is

$$f(t) = \exp\left[-\tfrac{1}{2}\gamma v_\perp t - \frac{\Delta_0}{\gamma v_\perp} e^{-\gamma v_\perp t}\right] . \tag{A1}$$

Let

$$\Lambda \equiv \frac{\Delta_0}{\gamma v_\perp} . \tag{A2}$$

Changing the variables of integration $t$ and $t'$ in the third term of Eq. (8) to ones proportional to $t - t'$ and $t + t'$ gives (with $y_c \equiv \gamma z_c$)

$$P = \langle n_a(0)\rangle e^{-2\Lambda} + \tfrac{1}{2}(1 - e^{-2\Lambda}) - \frac{2\Lambda}{\pi}\int_0^\infty \frac{dx}{x}\int_x^\infty dy \exp(-y - 2\Lambda e^{-y}\cosh x)\sin\frac{2b(y - y_c)x}{\gamma^2 v_\perp} . \tag{A3}$$

With

$$\zeta \equiv \frac{2b}{\gamma^2 v_\perp} , \tag{A4}$$

we can write the third term in (A3) as

$$-\frac{2\Lambda}{\pi}\int_0^\infty \frac{dx}{x}\sum_{k=0}^\infty \frac{(-2\Lambda\cosh x)^k}{k!}\int_x^\infty dy\, e^{-(k+1)y}\sin\zeta x\,(y - y_c) .$$

Performing the $y$ integral in this term allows writing $P$ as[24]

$$P = \langle n_a(0)\rangle e^{-2\Lambda} + \tfrac{1}{2}(1 - e^{-2\Lambda}) - \frac{2\Lambda}{\pi}\,\mathrm{Im}\int_0^\infty \frac{dx}{x} e^{-i\zeta y_c x}(2\Lambda\cosh x)^{i\zeta x - 1}[\Gamma(1 - i\zeta x) - \Gamma(1 - i\zeta x, 2\Lambda e^{-x}\cosh x)] . \tag{A5}$$

The term involving the incomplete $\Gamma$ function is $O(e^{-\Lambda})$. If we neglect terms of this order, we obtain, since $\Gamma(1+z)=z\Gamma(z)$,

$$P=\tfrac{1}{2}+\frac{\zeta}{\pi}\,\mathrm{Re}\int_0^\infty \frac{dx}{\cosh x}(2\Lambda\cosh x)^{i\zeta x}e^{-i\zeta y_c x}\Gamma(-i\zeta x)\ . \tag{A6}$$

The limit discussed by Blandin, Nourtier, and Hone[1] in which $\epsilon_a(z)$ is $z$ independent can be recovered from this form by letting $z_c$ [the point at which $\epsilon_a(z)$ crosses $\epsilon_F$]$\to\infty$ and $b$ [slope of $\epsilon_a(z)$]$\to 0$ such that $E_0\equiv\epsilon_F-\epsilon_a(0)$ stays finite. Since $E_0=bz_c$ [Eq. (10)], we write the product $\zeta y_c$ in the factor $\exp(-i\zeta y_c x)$ here as $2E_0/\gamma v_\perp$. Because $\Gamma(z)\sim z^{-1}$ for small $z$, we have, for $\zeta\to 0$ (recall $\zeta\propto b$),

$$P\to\tfrac{1}{2}+\frac{1}{\pi}\int_0^\infty \frac{dx}{x\cosh x}\sin\frac{2E_0}{\gamma v_\perp}x\ . \tag{A7}$$

This is Eq. (59) of Ref. 1. Now we discuss the form given in Eq. (13) in the text, obtained for $\zeta\to\infty$. This form omits terms of $O(e^{-2\Lambda})$. With the definition

$$W\equiv\ln\frac{2\Delta(z_c)}{\gamma v_\perp}\ , \tag{A8}$$

it is convenient to write (A5) as [omitting terms of $O(e^{-2\Lambda})$]

$$P=\tfrac{1}{2}-\frac{1}{\pi}\,\mathrm{Im}\int_0^\infty \frac{dx}{x\cosh x}e^{i\zeta x(W+\ln\cosh x)}[\Gamma(1-i\zeta x)-\Gamma(1-i\zeta x,2\Lambda e^{-x}\cosh x)] \tag{A9}$$

(note that $W>0$ for the parameter range of interest). For $\zeta\to\infty$, the factor $\exp(-i\zeta Wx)$ in the integrand oscillates rapidly, and we can take $x\to 0$ in the slowly varying parts of the integrand. Thus [with $u=-\zeta x$ (where we take $\zeta>0$, which is appropriate for the negative-ion case considered here), and continuing to omit terms of $O(e^{-2\Lambda})$],

$$P\to\tfrac{1}{2}+\frac{1}{\pi}\,\mathrm{Re}\int_{-\infty}^0 du\,e^{-iWu}\Gamma(iu)\ . \tag{A10}$$

This is most conveniently evaluated using contour integration with a contour that runs along the negative real axis and the positive imaginary axis in the complex $u$ plane, and is closed by a quarter circle at infinity. Employing the fact that $\Gamma(z)$ has simple poles at $z=-l$ (where $l=0,1,2,\ldots$),[25] with residues $(-1)^l/l!$, it is seen that

$$P=e^{-e^W}=e^{-2\Delta(z_c)/\gamma v_\perp}\ . \tag{A11}$$

## APPENDIX B: SPUTTERED ATOM TRAJECTORY WITH MORSE-POTENTIAL INTERACTION

We consider in this appendix the trajectory of an adsorbed atom of mass $m$ interacting with a single substrate atom of mass $M$ via the potential $U(s)$ given in Eq. (27) ($s$ is the interparticle distance). The substrate atom is considered to have received a sudden impulse at $t=0$; the collision of the now-moving substrate atom with the adsorbed atom is taken to be head-on (along a line at angle $\theta$ with respect to the surface normal). For $t>0$, the substrate-atom–adsorbed-atom pair is taken to have no interactions with any other atoms. We wish to find $r(t)$, the coordinate of the adsorbate atom along the line of collision; the quantity that enters the calculations of the ion probability $P$ is just[18] $z(t)=r(t)\cos\theta$. We take $r(0)=0$. Let $v_M(t)$ denote the velocity of the substrate atom along the line of collision with the adsorbate atom; and write $v_M\equiv v_M(0+)$ (i.e., the velocity just after the sudden impulse). Let $v_m(t)=dr(t)/dt$ denote the adsorbate atom velocity; $v_m(0+)=0$, and we write $v\equiv v_m(\infty)$.

For $t>0$, we write equations for conservation of energy [cf. Eq. (27)],

$$\tfrac{1}{2}mv_m(t)^2+\tfrac{1}{2}Mv_M(t)^2+U(s(t))=\tfrac{1}{2}Mv_M^2-\mathscr{E}\ , \tag{B1}$$

and conservation of momentum,

$$mv_m(t)+Mv_M(t)=Mv_M\ . \tag{B2}$$

Using Eqs. (27)–(29), we can thus eliminate $v_M(t)$ to write

$$v_m(t)^2-\frac{2v_M}{1+\delta}v_m(t)+v_{\mathscr{E}}^2[1-e^{-\beta(s(t)-s_0)}]^2=0\ . \tag{B3}$$

Since

$$\dot{s}(t)=v_m(t)-v_M(t)\ ,$$

Eq. (B2) also allows us to write

$$v_m(t)=\frac{v_M+\dot{s}(t)}{1+\delta}\ . \tag{B4}$$

Combining Eqs. (B3) and (B4) gives an equation for

$\dot{s}(t)$ which can be integrated to obtain

$$t=\pm\int ds[v_{\mathscr{E}}^2(1+\delta)^2(2e^{-\beta(s(t)-s_0)} -e^{-2\beta(s(t)-s_0)}) +v_M^2-v_{\mathscr{E}}^2(1+\delta)^2]^{-1/2} . \quad \text{(B5)}$$

Now for $v_M<v_{\mathscr{E}}(1+\delta)$, Eq. (B5) gives $s$ as a periodic function of time,[26] while for $v_M>v_{\mathscr{E}}(1+\delta)$, $s(t)\to\infty$ as $t\to\infty$ (i.e., the particles separate). We consider only the latter case, as noted in the text.

If we take $t\to\infty$ in Eq. (B3), then, since $s(t)\to\infty$ for the case we wish to consider, we can write

$$v_M=\tfrac{1}{2}(1+\delta)\left[v+\frac{v_{\mathscr{E}}^2}{v}\right] . \quad \text{(B6)}$$

It is also convenient to introduce the quantity

$$\bar{v}=[v_M^2-v_{\mathscr{E}}^2(1+\delta)^2]^{1/2} , \quad \text{(B7)}$$

thus the crossover from monotonically increasing behavior for $s(t)$ to periodic behavior occurs at $\bar{v}=0$. Using (B6) we can write

$$\bar{v}=\tfrac{1}{2}(1+\delta)\left[v-\frac{v_{\mathscr{E}}^2}{v}\right] ; \quad \text{(B8)}$$

so the crossover point corresponds to $v=v_{\mathscr{E}}$.

In terms of these quantities, we can write the solution for $s(t)$ obtained from Eq. (B5) as

$$s(t)=s_0+\bar{v}t+F(t) , \quad \text{(B9)}$$

where

$$F(t)=\frac{1}{\beta}\ln\frac{1}{2\bar{v}^2}[v_M(v_M-\bar{v})e^{-2\beta\bar{v}t} -2(v_M^2-\bar{v}^2)e^{-\beta\bar{v}t} +v_M(v_M+\bar{v})] . \quad \text{(B10)}$$

From Eq. (B4), we have

$$r(t)=[v_Mt+s(t)-s_0](1+\delta)^{-1} , \quad \text{(B11)}$$

and thus we obtain for the normal component of the sputtered-atom trajectory, for $v>v_{\mathscr{E}}$,

$$z(t)=[vt+(1+\delta)^{-1}F(t)]\cos\theta . \quad \text{(B12)}$$

---


[1]A. Blandin, A. Nourtier, and D. W. Hone, J. Phys. (Paris) 37, 369 (1976).

[2]J. K. Nørskov and B. I. Lundqvist, Phys. Rev. B 19, 5661 (1979).

[3]R. Brako and D. M. Newns, Surf. Sci. 108, 253 (1981); Vacuum 32, 39 (1982). The equation-of-motion approach used by Brako and Newns is that of W. Bloss and D. Hone, Surf. Sci. 72, 277 (1978).

[4]J. K. Nørskov, D. M. Newns, and B. I. Lundqvist, Surf. Sci. 80, 179 (1979).

[5]P. W. Anderson, Phys. Rev. 124, 41 (1961); D. M. Newns, *ibid.* 178, 1123 (1969).

[6]The term omitted from the expression for $P$ is

$$2\pi^{-1}\Delta_0 f(0)\mathrm{Re}\int_{-\infty}^{\epsilon_F}d\epsilon\{i[\epsilon-\epsilon_a(\vec{r}(0))]+\Delta_0\}^{-1}\int_0^{\infty}dt\,f(t)\exp\left[-i\int_0^t[\epsilon-\epsilon_a(\vec{r}(t'))]dt'\right] .$$

This can be evaluated by expressing the $\epsilon$ integral as an exponential integral, for which a continued-fraction form can be used.

[7]M. J. Lighthill, *Introduction to Fourier Analysis and Generalized Functions* (Cambridge University Press, Cambridge, England, 1964).

[8]Numerical evaluation of this integral is straightforward. The required values for the $\Gamma$ function can be computed using the recurrence relation for this function together with its asymptotic representation for arguments of large magnitude. See I. S. Gradshteyn and I. M. Ryzhik, *Table of Integrals, Series, and Products* (Academic, New York, 1965), 8.327 and 8.331.

[9]M. L. Yu, Phys. Rev. Lett. 47, 1325 (1981).

[10]N. D. Lang and A. R. Williams, Phys. Rev. B 18, 616 (1978). See also O. Gunnarsson, H. Hjelmberg, and J. K. Nørskov, Phys. Scr. 22, 165 (1980).

[11]Cf. R. W. Joyner and M. W. Roberts, Chem. Phys. Lett. 28, 246 (1974).

[12]D. E. Eastman, Solid State Commun. 10, 933 (1972); D. M. Hanson, R. Stockbauer, and T. E. Madey, Phys. Rev. B 24, 5513 (1981). These data are for adsorption on titanium; no data were found for a vanadium substrate.

[13]D. E. Eastman, Phys. Rev. B 2, 1 (1970).

[14]M. L. Yu, private communication.

[15]H. Hotop and W. C. Lineberger, J. Phys. Chem. Ref. Data 4, 539 (1975).

[16]N. D. Lang and W. Kohn, Phys. Rev. B 1, 4555 (1970).

[17]K. Y. Yu, J. N. Miller, P. Chye, W. E. Spicer, N. D. Lang, and A. R. Williams, Phys. Rev. B 14, 1446 (1976).

[18]A parallel-momentum effect discussed by D. M. Newns [Nordic Conference on Surface Science, Tampere, Finland, 1982 (unpublished)] is not important here because the sputtered-atom velocities (and thus their parallel components) are much smaller than the Fermi velocity.

[19]K. P. Huber and G. Herzberg, *Molecular Spectra and Molecular Structure—Volume 4: Constants of Diatomic Molecules* (Van Nostrand Reinhold, New York, 1979); E. U. Condon, in *Handbook of Physics,* 2nd ed., edited by E. U. Condon and H. Odishaw (McGraw-Hill, New York, 1967), Chap. 7, p. 108.

[20]U. Bänninger and E. B. Bas, Surf. Sci. 50, 279 (1975).

[21]In Fig. 6, for which the value $\mathscr{E}=9$ eV was used, the coordinates of the lower end of the 55° curve (marked by a dot) are $v_\perp=0.52\times10^6$ cm/sec and $\epsilon_0=0.29$ eV; had we used $\mathscr{E}=11.7$ eV, they would have been $v_\perp=0.59\times10^6$ cm/sec and $\epsilon_0=0.33$ eV.

[22]$E_0=6$ eV, $\Delta_0=1.5$ eV.

[23]M. L. Yu and N. D. Lang, Phys. Rev. Lett. 50, 127 (1983).

[24]Gradshteyn and Ryzhik, *Table of Integrals, Series, and Products,* Ref. 8, 8.354.2.

[25]Gradshteyn and Ryzhik, *Table of Integrals, Series, and Products,* Ref. 8, 8.310.2.

[26]Gradshteyn and Ryzhik, *Table of Integrals, Series, and Products,* Ref. 8, 2.266.